PAPER

Titanium dioxide and fluoropolymer-based coating for smart fabrics with antimicrobial and water-repellent properties†

Oratai Jongprateep,*[ab] Chitlada Mani-lata,[a] Yosita Sakunrak,[a] Krittanant Audcharuk,[a] Tithametha Narapong,[a] Kasidit Janbooranapinij,[a] Siraprapa Pitiphattharabun,[ac] Amornrat Lertworasirikul,[a] Apirat Laobuthee, [iD][a] Naris Thengchaisri,[d] Hiroharu Ajiro, [iD][e] Hiroaki Yoshida[e] and Gasidit Panomsuwan [iD] *[ab]

In the coronavirus disease 2019 pandemic, protective clothing is required for medical staff at risk of infection. This study proposes functional smart fabrics with antimicrobial and water-repellent properties, using titanium dioxide (TiO_2) and fluoropolymer-based precursors as coating materials. Experimental results indicated a uniform distribution of TiO_2 particles with an average size below 200 nm throughout the fabric. A zone of inhibition test revealed that the fabric inhibited bacterial growth, specifically of *Staphylococcus aureus* and *Klebsiella pneumoniae*, before and after 10 wash cycles of the fabric. In wetting angle measurements, the contact angles of water droplets on the fabric ranged from 120° to 139°. A water repellency test confirmed that the coated fabrics retained their water-repellent property after 10 wash cycles.

Introduction

Since the beginning of 2020, the coronavirus disease 2019 (COVID-19) has been spreading globally. The number of active patients continues to increase, whereas the sufficiency of medical gowns, scrub suits, and surgical masks declines. When efficient protective gowns are scarce, medical staff are potentially exposed to infection and the spread of COVID-19 can accelerate. Water repellency and antimicrobial efficacy enhance the efficiency of preventative clothing against COVID-19 infection. Thus, the development of clothing with simultaneous antimicrobial efficacy and water repellency is required.

Metal oxides are effective against bacteria, fungi, algae, protozoa, and viruses.[1] Due to its high reactivity, nontoxicity, chemical stability, and low cost, titanium dioxide (TiO_2) is exploited in various applications including cosmetics, food coloring, photovoltaic cells, catalytic hydrogenation and degradation of organic pollutants, and antimicrobial applications.[2] The microbial killing ability of TiO_2 was demonstrated by Fujishima and Honda[3] and Tsuang *et al.*[4] The efficiency of TiO_2 in catalytic and antimicrobial activities is thought to be significantly influenced by the chemical composition and particle size of the catalyst.[5] The size of the active reaction sites is a crucial affecter of catalyst efficiency. Especially, increasing the specific surface area enhances the photocatalytic and antimicrobial reactivity of catalysts.[6,7] For this reason, TiO_2 nanoparticles are favorable for photocatalytic and antimicrobial applications.

Chemical composition also affects the photocatalytic and antimicrobial performance of TiO_2. As a polymorphic material, TiO_2 comprises three crystal structures: anatase (tetragonal), rutile (tetragonal), and brookite (orthorhombic). The existence of different TiO_2 phases reportedly influences the chemical reaction and efficiency of the catalytic performance. The most stable form of TiO_2 is rutile, with a lower energy bandgap than the other phases. Brookite is orthorhombic, difficult to synthesize, and the least stable phase. Therefore, it is unattractive for catalytic applications. Anatase is more reactive than rutile despite its larger bandgap energy. The high efficacy of anatase may be explained by the nature of its valence band and charge transport.[8] When anatase absorbs light, its valence band maximum can move to energy levels above the redox potentials of the adsorbed molecules, thus enhancing the electron transfer from TiO_2 to the adsorbed molecules.[9] Additionally, the bandgap of anatase is usually indirect, whereas that of rutile is direct. An indirect bandgap prolongs the charge–carrier life

[a]*Department of Materials Engineering, Faculty of Engineering, Kasetsart University, Bangkok, Thailand. E-mail: gasidit.p@ku.ac.th; fengotj@ku.ac.th*

[b]*International Collaborative Education Program for Materials Technology, Education, and Research (ICE-Matter), ASEAN University Network, Southeast Asia Engineering Education Development Network (AUN/SEED-Net), Bangkok, Thailand*

[c]*Program of Sustainable Energy and Resources Engineering, Faculty of Engineering, Kasetsart University, Bangkok, Thailand*

[d]*Department of Companion Animal Clinical Sciences, Faculty of Veterinary Medicine, Kasetsart University, Chatuchak, Bangkok, Thailand*

[e]*Division of Materials Science, Nara Institute of Science and Technology, Ikoma, Nara, Japan*

† Electronic supplementary information (ESI) available. See DOI: 10.1039/d1ra05634d

time, enabling superior surface reactions. The charge-transport process is further enhanced by the much lower polaron effective mass of anatase than of rutile. Despite demonstrating superior catalytic efficiency, single-phase anatase may not exhibit the highest efficacy. Synergic effects on photocatalytic performance have been reported in mixed rutile-and-anatase-phase TiO_2.[10] The commonest commercial TiO_2 used in catalytic applications is Degussa P-25, which also contains rutile and anatase phases.

The fluid-repellent properties of materials are usually tested in water. Water repellency can be introduced by hydrophobic surface treatments that reduce the free surface energy of the fabric.[11] Water repellency is often enhanced by surface treatment agents such as paraffin, fatty acid resins, silicone-based compounds, and fluoropolymers.[12] Paraffin emulsion coatings are readily available at relatively low cost but have poor durability and may increase the flammability of fabrics. Fabrics coated with fatty acid resin is also reported to have poor durability. Some types of silicone-based water-repellent coatings have high durability, softness, improved sewing ability, and good appearance, but when applied in multiple layers, show low hydrophobicity. Additionally, excessively thick silicone-based coating layers may exacerbate pilling, seam slippage, and attraction of hydrophobic dirt. Acrylate and polyurethane with fluorinated side chains are common fluoropolymers used as water-repellent chemicals. Some fluoropolymer coatings exhibit simultaneous hydrophobic and oleophobic properties, preventing not only water penetration, but also the penetration of cooking fat, waste oil, and human secretions.[13]

Wettability is conventionally assessed by measuring the contact angle of water on the material surface. The contact angle, which is strongly related to water repellency, is influenced by the difference between the surface energies of the fabric and water (or its vapor). Hydrophobic materials are generally characterized by contact angles of 90° or higher. The water permeability or nonpermeability of fabrics can also be determined in hydrostatic pressure tests (AATCC 127 standard developed by the American Textile Chemists and Colorists Association)[14] and spray tests (AATCC 22 standard).[15] Fabric resistance to blood is tested using synthetic blood (ISO 15503).

The present work introduces a simple technique for producing smart fabrics with antimicrobial and water-repellent properties. To promote these properties, the fabrics were coated with TiO_2 photocatalysts and fluoropolymer-based solutions. The presence of TiO_2 was confirmed in scanning electron microscopy (SEM) images of the fabric surface morphology. Water repellency was evaluated in water contact angle measurement and spray tests. The antibacterial property was tested on Gram-positive *Staphylococcus aureus* and Gram-negative *Klebsiella pneumonia*. To test the durability of the coating, the water repellency and antimicrobial properties of the coated fabric were re-evaluated after 10 wash cycles.

Experimental

Materials

The fabric used in this work was made from Toray-Toteron Cotton (TC), which is a blend of polyester (65%) and cotton (35%). The chemical functional group of the fabric was confirmed by Fourier transform infrared spectrometer, as shown in Fig. S1.†

As the antimicrobial agent, we used multiphase TiO_2 comprising anatase-phase (A-TiO_2), rutile phase (R-TiO_2), and commercial Degussa P25 (P25, with 85% anatase and 15% rutile). Rutile TiO_2 powder (200 nm particle size) and Degussa P25 were purchased from Sigma Aldrich, and the anatase-phase was synthesized *via* the solution combustion technique. The aqueous solution for the combustion process was prepared from titanium(IV) isopropoxide (97%, Sigma Aldrich) and glycine (99% NH_2CH_2COOH, Fluka Analytical) as the initial reagent and combusting fuel, respectively. To ensure a homogeneous mixture, the solution was magnetically stirred and ultrasonically dispersed. The solution was heated to less than 400 °C to initiate combustion. After the combustion reaction, the powder products were collected and calcined at 400 °C for 2 h.

Polyvinylpyrrolidone (PVP, $(C_6H_9NO)_n$) was purchased from Krungthepchemi Co. Ltd. Polyvinyl alcohol (PVA, $CH_2CH(OH)_n$) was purchased from Sigma Aldrich. DARVAN® 821-a dispersing agent was purchased from Vanderbilt Minerals LLC. 691 Universal Duo Textile Stone (fluorine C-6, perfluorooctanoic acid-free), water soluble fluoropolymer, was purchased from Supreme Nanotech Ltd. Deionized (DI) water was used in all experiments, and all chemicals were used without further purification.

Preparation of TiO_2 slurry

The coating slurry was prepared from multiphase TiO_2 powders comprising A-TiO_2, R-TiO_2, and P25 (A-TiO_2 : R-TiO_2 : P25 = 3 : 1 : 1). Five grams of the TiO_2 powder was mixed with 2 L of DI water containing 0.625 g of dispersant, 0.9375 g of PVA, and 0.9375 g of PVP. The slurry was stirred vigorously at room temperature to ensure high uniformity and good dispersion.

Antimicrobial coating

The fabrics were coated *via* immersion in the TiO_2 slurry for 5 min. After soaking and squeezing, the fabrics were air-dried under ambient conditions for 24 h and then hot-dried by ironing (~1 kN m^{-2}, 103 ± 2 °C). The TiO_2 coating was carried out using a similar procedure for three times.

Water-repellent coating

The fluoropolymer solution was sprayed over the fabric surface and air-dried at room temperature for 24 h. Heat treatment was
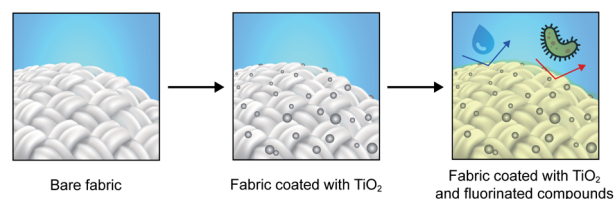

Fig. 1 Schematic showing the overall coating process of the photocatalyst and fluoropolymer on fabric.

Bare fabric   Fabric coated with TiO_2 Fabric coated with TiO_2 and fluorinated compounds

applied by ironing. The process was performed twice to complete the water-repellent coating. The overall coating process is depicted in Fig. 1.

Characterization

The phase structure of the TiO_2 powder was confirmed in a Philips X'Pert X-ray diffractometer with a Cu K_α radiation source. The 2θ range was 10–80°, the scan rate was 3° min^{-1}, and the step size was 0.01°. The fabric was trimmed into 3 cm × 3 cm squares for characterization. The surface morphology of the fabrics was observed on a Hitachi HU3500 SEM. The dispersions of TiO_2 powders and fluorinated compounds on the fabric surface were investigated *via* elemental mapping analysis using an Oxford energy-dispersive spectrometer.

The wettability of the fabric surface before and after coating was examined by water angle measurements. A 5 μL water drop was deposited on the surface and imaged at 10 s intervals. The contact angle was measured on six areas and averaged to give the final result. Contact angle measurements were repeated after 1, 3, and 10 wash cycles to examine the durability of the water-repellent coating. The wash process conformed to the AATCC TM 135: 2010 standard.

The durability of the water-repellent coating was evaluated in a water permeability spray test following the AATCC 22 test method. The resistance to blood penetration was tested using synthetic blood in an ISO 16603: 2004 test apparatus. The antimicrobial property of the coated fabric was tested *via* the growth analysis of *S. aureus* (ATCC 6538) and *K. pneumonia* (ATCC 4352) colonies.

Mechanical properties of fabric with and without coating, including Young's modulus and tensile strength, were measured on a Hounsfield H50KS universal testing machine. The fabrics were trimmed into a dimension of 2 cm × 10 cm in two different directions (weft and warp). The fabrics without and with coating were tested along with weft and warp directions, at a constant load of 900 N and a tension speed of 50 mm min^{-1} with 50 mm distance between clamps. Young's modulus and tensile strength were averaged from 10 specimens tested.
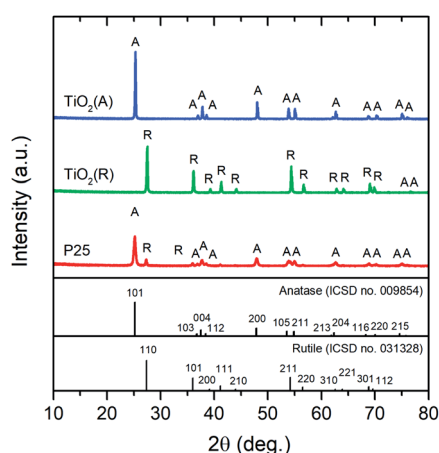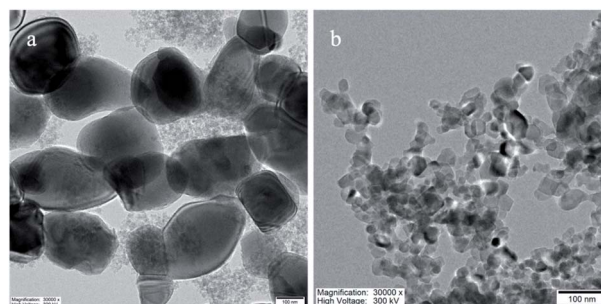

Fig. 3 TEM images of (a) A-TiO_2 and (b) P25.

Results and discussion

Characteristic of TiO_2 photocatalysts

The phase structure and microstructure of the TiO_2 photocatalysts used in the coating process were investigated using XRD and SEM analyses. The sharp peaks in the XRD patterns of A-TiO_2 and R-TiO_2 correspond to single-phase anatase (ISCD no. 009854) and rutile (ISCD no. 031328), respectively (Fig. 2). Meanwhile, the patterns of P25 presented the signals of both anatase and rutile, consistent with An *et al.*[16] The sharp diffraction peaks of all XRD patterns indicated highly crystalline TiO_2.

The transmission electron micrographs of the A-TiO_2 and P25 photocatalysts are displayed in Fig. 3a and b, respectively. The particles of both photocatalysts were irregularly shaped with average sizes of 181 ± 52 and 26 ± 9 nm, respectively. The fine sizes of the TiO_2 antimicrobial reagents might enhance the number of reactive sites and improve the antimicrobial performance.

Surface morphology of uncoated and coated fabrics

The morphologies of the fabrics before and after coating were investigated *via* SEM (see Fig. 4). The fibers of the noncoated fabric were smooth with no evidence of nanoparticles (Fig. 4a). After the first coating, TiO_2 particles were scarcely observed on the fiber surface (Fig. 4b). After successive coatings, TiO_2 particles were frequently observed and uniformly distributed on
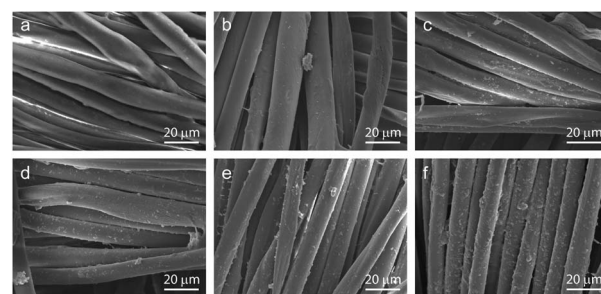

Fig. 4 SEM images of the fabric after successive coatings of TiO_2: (a) zero coating (bare fabric), (b) one coating, (c) two coatings, and (d) three coatings; (e) and (f) TiO_2-coated fabric after one and two coatings with fluoropolymer, respectively.

Fig. 2 XRD patterns of the three types of TiO_2 used in this work.
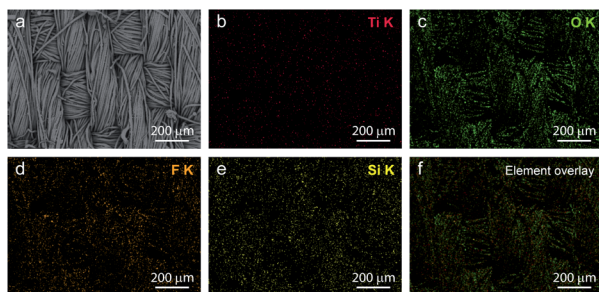
Fig. 5 Elemental mapping images of the coated fabric: (a) SEM image; distributions of (b) Ti, (c) O, (d) F, (e) Si, and (f) element overlay.

the fiber surface, resulting in rougher surface, as shown in Fig. 4c and d.

After coating with fluorinated compound, a thin layer was formed covering the fiber surface, resulting in a rougher surface. The presence of both TiO_2 and fluorinated compounds on the coated fabrics was confirmed using energy-dispersive elemental (EDS) mapping analysis (see Fig. 5). The signals of Ti, F and Si elements were uniformly detected over the investigated area. The Ti, F, and Si contents increased with the increasing number of coatings. Together, the SEM and EDS mapping data confirm that both TiO_2 and the fluorinated compounds were uniformly coated on the fabric surface. In addition, the presence of Si element indicates the presence of silane coupling agent in the solvent of fluorinated compound.

The amount of TiO_2 coated on fabrics was measured and confirmed by measuring the weight of fabrics before and after coating at different cycles (Table S1 and Fig. S3†). After one coating of TiO_2, the weight increased by about $1.33 \pm 0.58\%$. Their weight continuously increased to $2.50 \pm 0.57\%$ and $3.46 \pm 0.75\%$ after two and three coatings of TiO_2, respectively. However, the weight gain after two and three coatings was found to be lower as compared to one coating. This result was because TiO_2 were both leached and deposited on fabric during soaking, which resulted in a slight change in weight after two and three coatings. Although weight gain after coating was not exactly equal to the actual amount of TiO_2, it implied the increase of TiO_2 on the fabric after successive coating since the PVP and PVA had less contributions (Table S2†). The TiO_2 particles could adhere to the fabric by several possible interactions, such as van der Waal force, electrostatic force with surface functional groups (*e.g.*, carbonyl, hydroxyl, and carboxylic groups), and entrapment inside pores of fibers or intra-yarn pores.[17,18]
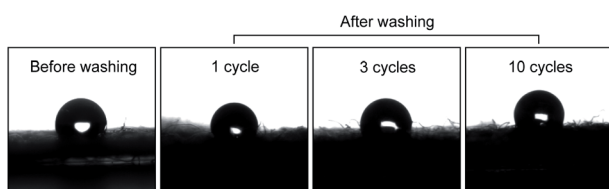
Table 1 Contact angles on the coated fabric before and after washing

Sample	Contact angle at 0 s	Contact angle at 60 s
Before washing	132.0°	130.4°
After 1 wash cycle	120.4°	118.5°
After 3 wash cycles	129.4°	124.5°
After 10 wash cycles	131.4°	122.1°

Water repellency of the coated fabrics

The water repellencies of the coated fabrics before washing and after 1, 3, and 10 wash cycles were determined from the contact angles of a water droplet on the fabric surface. The results are shown in Fig. 6 and summarized in Table 1. As mentioned above, the larger the contact angle, the higher was the hydrophobicity. Before washing, the contact angle on the coated fabric was ~132°, slightly decreasing to 130.4° after 60 s, confirming the poor wettability (excellent water repellency) of the coated fabric.[19]

After one wash cycle, the contact angle decreased to 120.4° because the fluorinated compounds were leached during washing. Leaching was confirmed by the decreased F content in an EDS analysis of the washed fabric. Unexpectedly, the contact angles recovered after three and 10 wash cycles, possibly because the fabric was roughened by crushing destruction of the fibers during the washing process. Roughening the surface of a material is known to enhance its hydrophobicity.

As confirmed in the contact angle measurements, the water repellency was slightly reduced after washing. The durability of the water-repellent coating was verified in a spray test (AATCC 22), which measures the wetting degree when the fabric is drizzled by water. The water stain characteristics at different wetting degrees (in ISO standard ratings) are listed in Table 2.

The wettability level of the uncoated fabric was 0, referring to no water repellency. After one coating of TiO_2, the wettability level was found to be 0, which was similar to uncoated fabric. However, the wettability level of the coated fabrics increased up to 50 after two coatings and remained the same value after three coatings. This result indicates that the water repellent property of the fabrics could be enhanced by increasing the number of TiO_2 coating. As revealed in the SEM images (Fig. 4c and d),

Table 2 Wettability levels specified in the AATCC 22 standard for spray tests[15]

Wettability level	Water stain characteristics
100 (ISO5)	No wetting of the specimen face
90 (ISO 4)	Slight random wetting of the specimen face
80 (ISO 3)	Wetting of specimen face at spray points
70 (ISO 2)	Partial wetting of the specimen face beyond the spray points
50 (ISO 1)	Complete wetting of the entire specimen face
0	Complete wetting of the entire face of the specimen

Fig. 6 Contact angle of a water droplet on the coated fabrics before washing and after 1, 3, and 10 wash cycles.
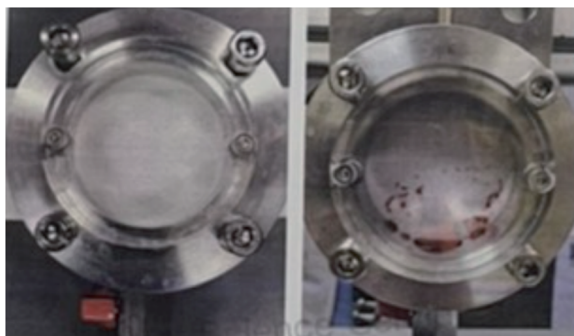
Fig. 7 Results of the blood penetration test: fragments of gown under an applied pressure of (left) 0 kPa and (right) 1.75 kPa.
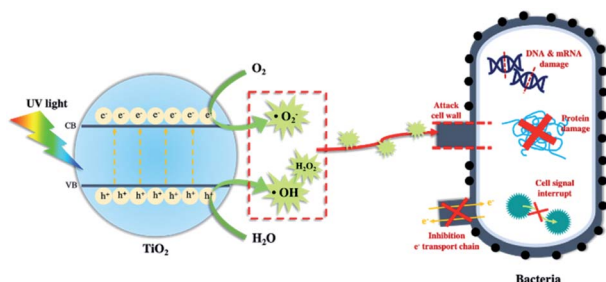

Fig. 8 Schematic of antibacterial mechanisms of TiO$_2$.

TiO$_2$ particles created a rougher surface on fibers, which could result in the development of a weak hydrophobic surface.[20–22] Water repellent property was greatly enhanced in the fabric coated with a fluoropolymer. Fabric coated with fluoropolymer exhibited a wettability level as high as 70–75. Wettability level still remained some of its original water repellency of 70–75 after washing for 10 cycles. The water stain characteristics were categorized wettability level of 70 as "partial wetting of the specimen face beyond the spray points". The wettability level of uncoated and all coated fabrics with different conditions are summarized in Table S3.† A wettability level of 70 (ISO-2) is the general performance requirement for raincoats, trench coats, jackets, and outerwears. Moreover, the water repellency of the coated fabrics endured multiple wash cycles. Rowen and Gagliardi[23] considered that when the water repellency is slightly diminished by laundering, a fabric is durably resistant to water.
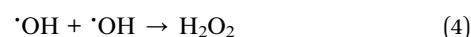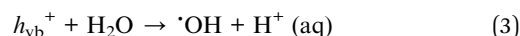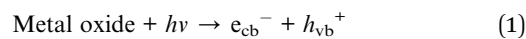
Furthermore, the body fluid penetrations of the fabrics were tested using synthetic blood according to the ISO 16603: 2004 standard. The fabrics with an average thickness of 0.239 mm and an areal density of 1.258 g cm^{-2} passed the penetration test under no applied pressure but failed under a hydrostatic pressure of 1.75 kPa (see Fig. 7). Therefore, the fabric met only the requirement for Class 1 materials. These results suggest that the fabric can be worn during general procedures and biopsies but is inappropriate for intensive care units or surgical operations.[24]

Antibacterial property

Several antibacterial activities are mechanized *via* the synthesis inhibition of the cell wall, nucleic acids, proteins, or metabolic compounds. Others operate through membrane disruption or interruption of microbial respiration.[25] Metal oxides such as TiO$_2$ are well-known antimicrobial agents. In the presence of TiO$_2$, microbes generate reactive oxidizing species (ROS) such as hydroxyl radicals ($^{\cdot}$OH), peroxides, and superoxides (O$_2^-$), which inhibit respiratory chain activity and enzyme synthesis and destroy RNA/DNA, cell membranes, and cell walls.[26] (see Fig. 8).

ROS are generated when TiO$_2$ absorbs light of a certain wavelength, forming electron–hole pairs (eqn (1)). Electrons in the conduction band (e$_{cb}^-$) of TiO$_2$ react with oxygen molecules (O$_2$) to form O$_2^{-\cdot}$ (eqn (2)). Meanwhile, holes in the valence band (h$_{vb}^+$) react with H$_2$O, generating hydroxyl radicals ($^{\cdot}$OH) (eqn (3)). These hydroxyl radicals further react with each other to form hydrogen peroxide (H$_2$O$_2$) (eqn (4)).

$$\text{Metal oxide} + hv \rightarrow \text{e}_{cb}^- + h_{vb}^+ \tag{1}$$

$$\text{O}_2 + \text{e}_{cb}^- \rightarrow \text{O}^{2-\cdot} \tag{2}$$

$$h_{vb}^+ + \text{H}_2\text{O} \rightarrow {}^{\cdot}\text{OH} + \text{H}^+ \text{ (aq)} \tag{3}$$

$${}^{\cdot}\text{OH} + {}^{\cdot}\text{OH} \rightarrow \text{H}_2\text{O}_2 \tag{4}$$

The antimicrobial performances of the gowns were assessed following the AATCC TM 147: 2016 standard (Test Method for Antibacterial Activity of Textile Materials). AATCC TM is the normal qualitative approach for assessing the antibacterial activities of diffusible antimicrobial agents on textiles. The test organisms were Gram-positive *S. aureus* (ATCC 6538) and Gram-negative *K. pneumoniae* (ATCC 4352). A piece of fabric cut from the uncoated and coated fabrics was placed across streaks of the bacterial species on an agar plate. The uncoated fabric and only fluoropolymer coated fabrics showed zero zone inhibition against *S. aureus* and *K. pneumoniae*, indicating no

Table 3 Zones of inhibition of the uncoated and coated fabrics (AATCC TM 147: 2016 standard)

Specimen	Zone of inhibition (mm)	
	S. aureus (ATCC 6538)	*K. pneumoniae* (ATCC 4352)
Fabric without coating	0	0
Fabric coated with only fluoropolymer coating	0	0
Fabric coated with TiO$_2$ and fluoropolymer	4.9	2.5
Fabric coated with TiO$_2$ and fluoropolymer after washing 10 cycles	6.3	4.5

Table 4 Mechanical properties, including Young's modulus and tensile strength, of uncoated and coated fabrics along weft and warp directions

Direction	Specimen	Mechanical properties	
		Young's modulus (MPa)	Tensile strength (MPa)
Weft	Uncoated fabric	337.76 ± 7.80	47.29 ± 5.23
	Coated fabric	368.76 ± 13.78	68.40 ± 2.95
Warp	Uncoated fabric	175.01 ± 11.16	32.66 ± 1.23
	Coated fabric	186.40 ± 12.91	33.11 ± 2.76

antimicrobial property. On the contrary, no bacterial growths were observed under the fabrics coated with both TiO_2 and fluoropolymer; instead, a clear inhibition zone appeared. The inhibition zones against *S. aureus* and *K. pneumoniae* were 4.9 and 6.3 mm in diameter, respectively (see Table 3). These results clearly confirm the antimicrobial properties of TiO_2. To further evaluate the antimicrobial durability of the fabrics, the tests were repeated after 10 wash cycles. Similar results were obtained, although with slightly reduced zones of inhibition. The results elucidated the antimicrobial properties of the fabrics even after 10 wash cycles.

Mechanical properties

Mechanical properties of the fabrics before and after coating, including Young's modulus, yield strength, tensile strength, and elongation at break, are summarized in Table 4. Young's modulus and tensile strength of uncoated fabrics in the weft directions were better than those in the warp direction. After coating, the mechanical properties slightly increased in the warp direction but significantly increased in the weft direction. An improvement of the mechanical properties of coated fabrics in both directions could be explained as follows. Fluoropolymer, PVP, and PVA could fill in the interstices at the fiber–fiber region of spun yarn and also form as a thin layer on the yarn surface, providing additional strength to the fabrics.[27,28] Moreover, the presence of TiO_2 particles on the coated fabric may help bearing the external force and strengthening the fabric since TiO_2 is an inorganic mineral, which is stiffer than fabric.

Conclusions

Anatase-phase TiO_2 nanoparticles (smaller than 200 nm on average) were synthesized *via* the solution combustion technique and applied as antimicrobial agents. To enhance their efficacy, the synthesized TiO_2 powders were mixed with commercially available rutile TiO_2 and Degussa P-25. Medical gowns were coated by simple dip coating, drying, and ironing procedures. To ensure the durability of their antimicrobial performance and water repellency, the gowns were coated with two layers of TiO_2 and three layers of a fluorinated compound. Experimental results indicated that the TiO_2 particles were uniformly distributed throughout the fabrics. The fabric effectively inhibited the growth of *S. aureus* and *K. pneumoniae*, even after 10 wash cycles. The high wetting angles (120–139°) before and after washing for 10 cycles confirmed the high water

repellency of the fabrics. The wettability level (70–75) demonstrated that the coated fabrics retained a fair water-repelling ability after 10 wash cycles. The fabric coated in this work shows a promising and smart material with an antimicrobial functional surface with water repellency for use as protective clothing under the COVID-19 pandemic.

Author contributions

Conceptualization: O. Jongprateep, G. Panomsuwan, A. Lertworasirikul, A. Laobuthee, N. Thengchaisri; data curation: Y. Sakunrak, K. Audcharuk, T. Narapong, O. Jongprateep, G. Panomsuwan; formal analysis: K. Janbooranapinij, Y. Sakunrak, K. Audcharuk, T. Narapong, O. Jongprateep, G. Panomsuwan; funding acquisition: O. Jongprateep, G. Panomsuwan; investigation: K. Janbooranapinij, Y. Sakunrak, K. Audcharuk, T. Narapong; methodology: Y. Sakunrak, K. Audcharuk, T. Narapong, G. Panomsuwan, O. Jongprateep, A. Lertworasirikul; project administration: O. Jongprateep, G. Panomsuwan; resource: A. Lertworasirikul, O. Jongprateep, G. Panomsuwan; visualization: S. Pitiphattharabun, Y. Sakunrak, G. Panomsuwan; validation: G. Panomsuwan, O. Jongprateep, H. Ajiro, H. Yoshida; A. Lertworasirikul, A. Laobuthee; writing – original draft: C. Mani-lata, S. Pitiphattharabun; O. Jongprateep, G. Panomsuwan; writing – review & editing: H. Ajiro, H. Yoshida, A. Lertworasirikul, O. Jongprateep, G. Panomsuwan.

Conflicts of interest

There are no conflicts to declare.

Acknowledgements

Notes and references

1 U. Kadiyala, N. A. Kotov and J. S. VanEpps, *Curr. Pharm. Des.*, 2018, **24**, 896–903.
2 L. E. Oi, M. Y. Choo, H. V. Lee, H. C. Ong, S. B. A. Hamid and J. C. Juan, *RSC Adv.*, 2016, **6**, 108741–108754.
3 A. Fujishima and K. Honda, *Nature*, 1972, **238**, 37–38.

4 Y. H. Tsuang, J. S. Sun, Y. C. Huang, C. H. Lu, W. H. S. Chang and C. C. Wang, *Artif. Organs*, 2008, **32**, 167–174.

5 O. Jongpreteep and R. Puranasamriddhi, *Mater. Today: Proc.*, 2018, **5**, 10925–10931.

6 Y. Hu, H. L. Tsai and C. L. Huang, *J. Eur. Ceram. Soc.*, 2003, **23**, 691–696.

7 S. E. Jin and H. E. Jin, *Pharmaceutics*, 2021, **13**, 222.

8 T. Luttrell, S. Halpegamage, J. Tao, A. Kramer, E. Sutter and M. Batzill, *Sci. Rep.*, 2014, **4**, 4043.

9 M. Batzill, *Energy Environ. Sci.*, 2011, **4**, 3275–3286.

10 W. R. Siah, H. O. Lintang, M. Shamsuddin and L. Yuliati, High Photocatalytic Activity of Mixed Anatase–Rutile Phases on Commercial TiO$_2$ Nanoparticles, *IOP Conf. Ser.: Mater. Sci. Eng.*, 2016, **107**, 012005.

11 M. Montazer and T. Harifi, Water-Repellent Textile Nanofinishes, *Nanofinishing of Textile Materials*, Woodhead Publishing, 2018, The Textile Institute Book Series.

12 A. Krishnan, R. Gettu, R. Dhamodharan and P. S. Nair, *Int. J. 3R's*, 2013, **4**, 595–601.

13 A. Moiz, R. Padhye and X. Wang, *Coatings*, 2018, **8**, 104.

14 *AATCC Test Method 127, Water resistance: Hydrostatic pressure test*, American Association of Textile Chemists and Colorists, Research Triangle Park, 2017.

15 *AATCC Test Method 22, Water resistance: Hydrostatic pressure test*, American Association of Textile Chemists and Colorists, Research Triangle Park, 2017.

16 X. An, H. Liu, J. Qu, S. J. A. Moniz and J. Tang, *New J. Chem.*, 2015, **39**, 314.

17 M. Dhananjeyan, E. Mielczarski, K. Thampi, P. Buffet, M. Bensimon, A. Kulik, J. Mielczarski and J. Kiwi, *J. Phys. Chem. B*, 2001, **105**, 12046–12055.

18 M. Radetić, *J. Photochem. Photobiol. C Photochem. Rev.*, 2013, **16**, 62–76.

19 J. T. Simpson, S. R. Hunter and T. Aytug, *Rep. Prog. Phys.*, 2015, **78**, 086501.

20 C.-H. Xue, S.-T. Jia, H.-Z. Chen and M. Wang, *Sci. Technol. Adv. Mater.*, 2008, **9**, 035001.

21 S. Afzal, W. A. Daoud and S. J. Langford, *J. Mater. Chem. A*, 2014, **2**, 18005.

22 D. W. Wei, H. Wei, A. C. Gauthier, Y. Jin and H. Xiao, *J. Bioresour. Bioprod.*, 2020, **5**, 1–15.

23 J. W. Rowen and D. Gagliardi, *J. Res. Natl. Inst. Stand. Technol.*, 1947, **38**, 103–117.

24 *Standard Test Methods of Textiles: Resistance to Surface Wetting-Spray Test, Thai Industrial Standard 121 Part 22-2552*, Thai Industrial Standards Institute (TISI): Ministry of Industry (Thailand), 2010.

25 A. Erdem, D. Metzler, D. K. Cha and C. P. Huang, *Environ. Sci. Pollut. Res.*, 2015, **22**, 17917–17924.

26 C. L. de Dicastillo, M. G. Correa, F. B. Martínez, C. Streitt and M. J. Galotto, Antimicrobial Effect of Titanium Dioxide Nanoparticles, *Antimicrobial Resistance – A One Health Perspective*, IntechOpen, 2020.

27 B. Kim, V. Koncar and C. Dufour, *J. Appl. Polym. Sci.*, 2006, **101**, 1252–1256.

28 B. M. Kale, J. Wiener, J. Militky, S. Rwawire, R. Mishra, K. I. Jacob and Y. Wang, *Carbohydr. Polym.*, 2016, **150**, 107–113.